JOC*Note*

Mechanistic Insight into the Aromatic Hydroxylation by High-Valent Iron(IV)-oxo Porphyrin π-Cation Radical Complexes

Min-Jung Kang,[†] Woon Ju Song,[†] Ah-Rim Han,[†] Young S. Choi,[‡] Ho G. Jang,*[,‡] and Wonwoo Nam*[,†]

Department of Chemistry, Division of Nano Sciences, and Center for Biomimetic Systems, Ewha Womans University, Seoul 120−750, Korea, and Department of Chemistry and Center for Electro & Photo Responsive Molecules, Korea University, Seoul 136-701, Korea

wwnam@ewha.ac.kr; hgjang@korea.ac.kr

Received April 1, 2007

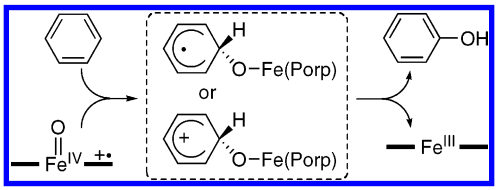

Mechanistic studies of the aromatic hydroxylation by high-valent iron(IV)-oxo porphyrin π-cation radicals revealed that the aromatic oxidation involves an initial electrophilic attack on the π-system of the aromatic ring to produce a tetrahedral radical or cationic σ-complex. The mechanism was proposed on the basis of experimental results such as a large negative Hammett ρ value and an inverse kinetic isotope effect. By carrying out isotope labeling studies, the oxygen in oxygenated products was found to derive from the iron-oxo porphyrin intermediates.

Aromatic hydroxylation is an important chemical process in enzymatic reactions, as evidenced by the detoxification processes and drug metabolism by Cytochromes P450, nonheme iron mono- and dioxygenases, and copper enzymes.[1−3] The aromatic hydroxylation has been extensively investigated over the past three decades in Cytochromes P450 and iron porphyrin models, with the intention of understanding their reaction mechanisms and developing artificial catalysis that can be used in drug synthesis and biodegradation of environmental pollutants.[1] The mechanism of the aromatic hydroxylation has been proven to be quite complex, as shown in the proposed mechanisms of the aromatic ring hydroxylation by high-valent iron(IV)-oxo porphyrin π-cation radicals (the so-called Compound I) (Scheme 1). Early studies concluded that the hydroxylation of aromatic compounds occurs via an arene oxide formation (Scheme 1, pathway A).[4] More recent experimental evidence, however, has revealed that the aromatic oxidation does not proceed via the epoxide intermediate formation but occurs via the generation of a tetrahedral radical or cationic σ-complex (Scheme 1, pathway B).[5] Very recently, density functional theory (DFT) calculations of aromatic hydroxylation by Compound I have shown that the aromatic ring activation involves an initial electrophilic attack on the π-system of the aromatic ring to produce a radical or cationic species (Scheme 1, pathway B).[6,7] The evidence for the formation of radical cations by direct electron abstraction from aromatic compounds is still ambiguous (Scheme 1, pathway C),[8] but DFT calculations do not support the electron-transfer mechanism.[6] The hydrogen abstraction mechanism has been ruled out on the basis of experimental results, including a small kinetic isotope effect (KIE) value despite the high bond dissociation energy of aromatic C−H bonds, and computational calculations (Scheme 1, pathway D).[6,9,10]

SCHEME 1

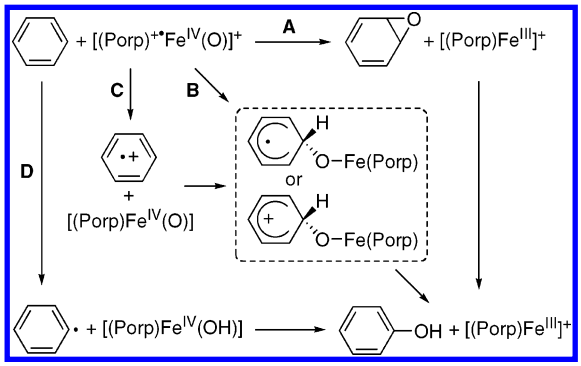

Since the previously proposed mechanisms were based on experimental results obtained under catalytic conditions and with an assumption that Compounds I were generated as reactive species in the catalytic reactions, we have investigated the aromatic hydroxylation by generating high-valent iron(IV)-oxo porphyrin π-cation radicals and using the intermediates directly

[†] Ewha Womans University.
[‡] Korea University.

(1) (a) de Montellano, P. R. O. *Cytochrome P450: Structure, Mechanism, and Biochemistry*, 3rd ed.; Kluwer Academic/Plenum Publishers: New York, 2005. (b) Meunier, B.; de Visser, S. P.; Shaik, S. *Chem. Rev.* **2004**, *104*, 3947−3980. (c) Meunier, B. In *Biomimetic Oxidations Catalyzed by Transition Metal Complexes;* Imperial College Press: London, 2000; pp 171−214.

(2) (a) Solomon, E. I.; Brunold, T. C.; Davis, M. I.; Kemsley, J. N.; Lee, S.-K.; Lehnert, N.; Neese, F.; Skulan, A. J.; Yang, Y.-S.; Zhou, J. *Chem. Rev.* **2000**, *100*, 235−349. (b) Fitzpatrick, P. F. *Biochemistry* **2003**, *42*, 14083−14091. (c) Costas, M.; Mehn, M. P.; Jensen, M. P.; Que, L., Jr. *Chem. Rev.* **2004**, *104*, 939−986. (d) Nam, W. *Acc. Chem. Res.*, published online May 2007, http://dx.doi.org/10.1021/ar700027f.

(3) (a) Lewis, E. A.; Tolman, W. B. *Chem. Rev.* **2004**, *104*, 1047−1076. (b) Land, E. J.; Ramsden, C. A.; Riley, P. A. *Acc. Chem. Res.* **2003**, *36*, 300−308.

(4) (a) Jerina, D. M.; Daly, J. W. *Science* **1974**, *185*, 573−582. (b) Jerina, D. M.; Daly, J. W.; Witkop, B.; Zaltzman, P.; Udenfriend, S. *J. Am. Chem. Soc.* **1968**, *90*, 6525−6527.

(5) (a) Vannelli, T.; Hooper, A. B. *Biochemistry* **1995**, *34*, 11743−11749. (b) Korzekwa, K. R.; Swinney, D. C.; Trager, W. F. *Biochemistry* **1989**, *28*, 9019−9027. (c) Burka, L. T.; Plucinski, T. M.; MacDonald, T. L. *Proc. Natl. Acad. Sci. U.S.A.* **1983**, *80*, 6680−6684.

(6) De Visser, S. P.; Shaik, S. *J. Am. Chem. Soc.* **2003**, *125*, 7413−7424.

(7) (a) Bathelt, C. M.; Ridder, L.; Mulholland, A. J.; Harvey, J. N. *J. Am. Chem. Soc.* **2003**, *125*, 15004−15005. (b) Bathelt, C. M.; Ridder, L.; Mulholland, A. J.; Harvey, J. N. *Org. Biomol. Chem.* **2004**, *2*, 2998−3005.

(8) (a) Sato, H.; Guengerich, F. P. *J. Am. Chem. Soc.* **2000**, *122*, 8099−8100. (b) Riley, P.; Hanzlik, R. P. *Xenobiotica* **1994**, *24*, 1−16.

(9) Hanzlik, R. P.; Ling, K.-H. J. *J. Am. Chem. Soc.* **1993**, *115*, 9363−9370.

(10) Shiota, Y.; Suzuki, K.; Yoshizawa, K. *Organometallics* **2005**, *24*, 3532−3538.

10.1021/jo070557y CCC: $37.00
Published on Web 07/10/2007

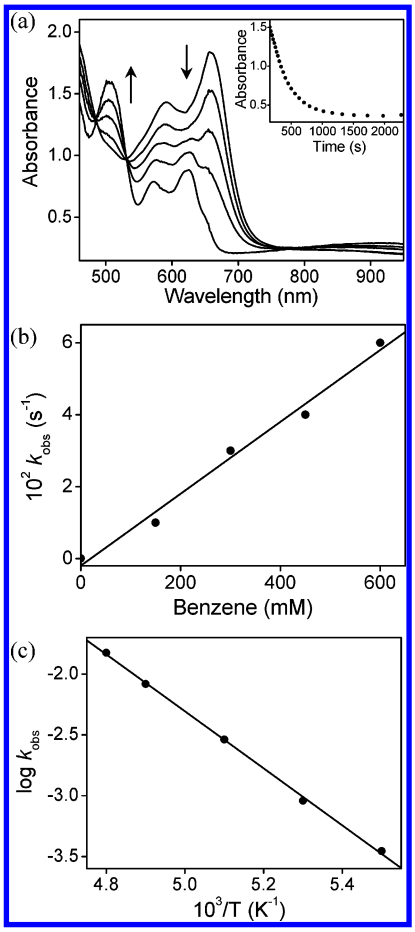

FIGURE 1. (a) UV−vis spectral changes of **1** (1.5 mM) upon addition of 100 equiv of benzene in CH_2Cl_2 at −80 °C. Inset shows absorbance traces monitored at 660 nm. (b) Plot of k_{obs} against benzene concentration to determine a second-order rate constant at −80 °C. (c) Plot of first-order-rate constants against 1/*T* to determine activation parameters.

in kinetic studies of aromatic hydroxylation under stoichiometric conditions. In this work, we have observed a large negative Hammett ρ value in the reactions of para-substituted benzenes and inverse KIE. By carrying out ^{18}O-labeling experiments, the oxygen in oxygenated products was found to derive from the iron-oxo porphyrin intermediates. To the best of our knowledge, this study provides the first mechanistic details of aromatic hydroxylation investigated with high-valent iron(IV)-oxo porphyrin π-cation radicals generated in situ.

A high-valent iron(IV)-oxo porphyrin π-cation radical complex, $[(TPFPP)^{+\bullet}Fe^{IV}(O)]^+$ (**1**) (TPFPP = *meso*-tetrakis(pentafluorophenyl)porphinato dianion) (Supporting Information, Figure S1 for the structure of iron porphyrins),[11] was prepared by treating Fe(TPFPP)(CF_3SO_3) with *m*-chloroperbenzoic acid (*m*-CPBA) in CH_2Cl_2 containing a small amount of CH_3CN at −80 °C. Upon addition of benzene to the solution, the intermediate reverted back to the starting iron porphyrin complex and showed pseudo-first-order decay as monitored by a UV−vis spectrophotometer (Figure 1a). Pseudo-first-order fitting of the kinetic data allowed us to determine the k_{obs} value to be $3.0(3) \times 10^{-3}$ s^{-1} (Figure 1a, inset). The pseudo-first-order rate constants increased proportionally with benzene concentration, thus leading us to determine a second-order rate constant to be $1.0(1) \times 10^{-1}$ $M^{-1}\cdot s^{-1}$ (Figure 1b). Activation parameters for the benzene hydroxylation was determined by plotting first-order-rate constants measured at different temperatures (183−208 K) against 1/T (Figure 2c); the activation enthalpy and entropy values were calculated to be $\Delta H^{\ddagger} = 4.6(3)$ kcal·mol^{-1} and $\Delta S^{\ddagger} = -29(2)$ cal·$mol^{-1}\cdot K^{-1}$, respectively. Product analysis of the benzene hydroxylation with GC and GC−MS revealed that benzoquinone was produced as a major product (vide infra).

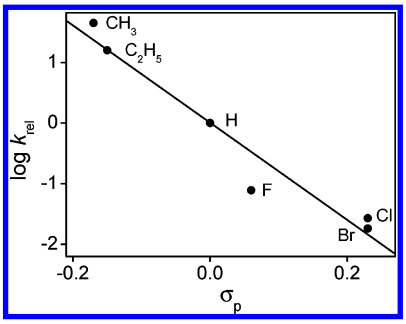

FIGURE 2. Hammett plot of log k_{rel} against σ_p of para-X-substituted benzenes. The k_{rel} values were calculated by dividing k_2 of para-X-benzene by k_2 of benzene.

We then investigated the electronic effect of benzene substrate on reaction rates, by carrying out the reactions of **1** with various para-X-substituted benzenes at −80 °C. The second-order rate constants were determined under the conditions described above but with different concentrations depending on their relative reactivities (Supporting Information, Figure S2). The data in Table S1 (Supporting Information) indicate that the electron-donating ability of the para substituents influences the reaction rate significantly. By plotting the second-order rates as a function of σ_p of the para substituents, a good linear correlation was obtained with a large negative Hammett ρ value of −8.0 (Figure 2), indicating an unusually high charge separation and electrophilic nature in the transition state of the benzene oxidation by iron(IV)-oxo porphyrin π-cation radical species. Further, such a large negative ρ value of −8.0 suggests the generation of a cationic species rather than a radical species in the transition state (see Scheme 1).[6]

It is worth noting that Hammett ρ values reported previously in the catalytic oxidation of aromatic compounds by Cytochrome P450 and iron(III) porphyrins are much smaller (ρ value of −1) than the value determined kinetically with iron(IV)-oxo porphyrin π-cation radicals generated in situ.[8b,12] Further, it is of interest to compare Hammett ρ values obtained in the aromatic hydroxylation and olefin epoxidation reactions.[11,13,14] In olefin epoxidations, ρ values of −1.8 and −1.9 were reported in the competitive epoxidation of para-substituted styrenes by **1** and in the kinetic studies of para-substituted styrenes by $[(TMP)^{+\bullet}Fe^{IV}(O)]^+$ (TMP = *meso*-tetramesitylporphinato dianion), respectively.[11,13] Such a large difference between the ρ

(11) We have shown very recently that iron(IV)-oxo porphyrin π-cation radicals prepared from their triflate iron porphyrins favor aromatic ring oxidation over C−H hydroxylation and that CH_3CN, which was used as a co-solvent in reaction solutions, might be coordinated as an axial ligand trans to the iron-oxo group: Song, W. J.; Ryu, Y. O.; Song, R.; Nam, W. *J. Biol. Inorg. Chem.* **2005**, *10*, 294−304.

(12) Khavasi, H. R.; Safari, N. *J. Mol. Catal. A: Chem.* **2004**, *220*, 127−132.

(13) Groves, J. T.; Watanabe, Y. *J. Am. Chem. Soc.* **1986**, *108*, 507−508.

(14) (a) Traylor, T. G.; Xu, F. *J. Am. Chem. Soc.* **1988**, *110*, 1953−1958. (b) Lindsay Smith, J. R.; Sleath; P. R. *J. Chem. Soc., Perkin Trans. 2* **1982**, 1009−1015.

TABLE 1. Kinetic Isotope Effect in the Hydroxylation of Aromatic Compounds by High-Valent Iron(IV)-oxo Porphyrin π-Cation Radical Complexes[a]

benzene hydroxylation by **1**			toluene hydroxylation by **2**			naphthalene hydroxylation by **3**		
rate constant[b] (10^{-1} s^{-1})			rate constant[b] (10^{-3} s^{-1})			rate constant[b] (10^{-2} s^{-1})		
C_6H_6	C_6D_6	k_H/k_D	C_7H_8	C_7D_8	k_H/k_D	$C_{10}H_8$	$C_{10}D_8$	k_H/k_D
0.8	1.0	0.8	1.8	2.2	0.82	0.8	1	0.8

[a] Reactions were done with $[(TDCPP)^{+\bullet}Fe^{IV}(O)]^+$ (1.5 mM) and substrates (15 mM for benzene, 150 mM for toluene, and 15 mM for naphthalene) in CH_2Cl_2 at −80 °C. Rate constants are averaged by three determinations.

values of aromatic hydroxylation and olefin epoxidation is attributable to the involvement of a more polar species in the transition state of aromatic hydroxylation, as Shaik and coworkers proposed in theoretical studies that a major difference between benzene hydroxylation and olefin epoxidation is the appearance of a cationic pathway in the case of benzene, whereas radicalar-only pathways operate in the case of olefins.[6,15]

Kinetic isotope effect (KIE) was also investigated kinetically in the hydroxylation of undeuterated and deuterated aromatic compounds by high-valent iron(IV)-oxo porphyrin π-cation radicals, such as in the reactions of benzene and deuterated benzene by **1**, toluene and deuterated toluene by $[(TDFPP)^{+\bullet}Fe^{IV}(O)]^+$ (**2**) (TDFPP = *meso*-tetrakis(2,6-difluorophenyl)porphinato dianion), and naphthalene and deuterated naphthalene by $[(TDCPP)^{+\bullet}Fe^{IV}(O)]^+$ (**3**) (TDCPP = *meso*-tetrakis(2,6-dichlorophenyl)porphinato dianion) (Table 1). The calculated k_H/k_D value of ∼0.8 indicates an inverse KIE in the aromatic ring oxidation reactions; the observation of the inverse KIE is consistent with the sp^2-to-sp^3 hybridization change during the addition of an electrophilic iron-oxo species to the sp^2 center of aromatic ring to form a σ adduct.[5a,6,9,16] Further, the inverse KIE rules out the hydrogen abstraction mechanism;[9] large KIE values ranging from 5 to 14 are observed in C−H bond activation by high-valent iron(IV)-oxo porphyrin π-cation radicals,[17] and we have reported a KIE value of 14 in cyclohexane hydroxylation by **1** at −80 °C.[11]

Finally, the source of oxygen in oxygenated products was investigated by carrying out isotope labeling studies in the hydroxylation of toluene by ^{18}O-labeled $[(TPFPP)^{+\bullet}Fe^{IV}(^{18}O)]^+$ (**1**-^{18}O) at −80 °C. To increase the accuracy of product analysis, the catalytic hydroxylation of toluene by $[Fe^{III}(TPFPP)]^+$ and PhIO was carried out in the presence of $H_2{}^{18}O$ at 25 °C. By analyzing the reaction solution with GC and GC−MS, we found that 2-methylbenzoquinone was produced as a major product (70% based on catalyst) with the formation of small amounts of 2- and 4-methylphenol (less than 5% based on catalyst) and that the percentages of M, M + 2, and M + 4 products were 9, 40, and 50%, respectively (Scheme 2).[18] The formation of quinone products has been well documented in aromatic

SCHEME 2

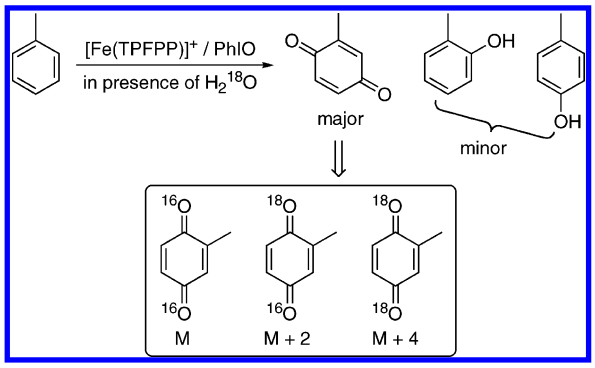

hydroxylation reactions catalyzed by metalloporphyrins,[19−21] and a mechanism has been proposed in which two metal-oxo complexes are needed for the formation of one quinone product.[19,20] The observation of the significant amount of ^{18}O-incorporation into the quinone product indicates that the source of the oxygen in the product is the iron-oxo porphyrin complex. However, since the product was not fully ^{18}O-labeled, we checked the percent of **1**-^{18}O generated in the labeled $H_2{}^{18}O$ experiments by carrying out the catalytic epoxidation of cyclohexene by $[Fe^{III}(TPFPP)]^+$ and PhIO under the identical conditions of the toluene hydroxylation.[22] In the latter experiment, we found that cyclohexene oxide contains 75% ^{18}O, indicating that 75% of **1** is labeled by ^{18}O. In control experiments, we checked that the oxygen of 2-methylbenzoquinone does not exchange with $H_2{}^{18}O$ under the conditions. Further, the product formed in the hydroxylation of toluene under $^{18}O_2$ atmosphere did not contain ^{18}O, demonstrating that O_2 is not involved in the toluene hydroxylation. Furthermore, the oxidation of phenol and *o*-cresol by **1** afforded only trace amounts of benzoquinone and 2-methylbenzoquinone, respectively, proposing that two high-valent metal-oxo molecules are simultaneously involved in producing the quinone products in the oxidation of aromatic compounds.[19a]

In summary, we have reported mechanistic details of aromatic hydroxylation investigated kinetically with high-valent iron(IV)-oxo porphyrin π-cation radicals generated in situ. On the basis of the experimental results of a large Hammett ρ value and an inverse KIE, we have proposed that the aromatic oxidation involves an initial electrophilic attack on the π-system of the aromatic ring to produce a tetrahedral radical or cationic σ-complex (Scheme 1, pathway B). We have also demonstrated

(15) (a) de Visser, S. P.; Ogliaro, F.; Harris, N.; Shaik, S. *J. Am. Chem. Soc.* **2001**, *123*, 3037−3047. (b) de Visser, S. P.; Ogliaro, F.; Sharma, P. K.; Shaik, S. *J. Am. Chem. Soc.* **2002**, *124*, 11809−11826.

(16) Griffin, G. W.; Horn, K. A. *J. Am. Chem. Soc.* **1987**, *109*, 4919−4926.

(17) (a) Kumar, D.; de Visser, S. P.; Sharma, P. K.; Cohen, S. Shaik, S. *J. Am. Chem. Soc.* **2004**, *126*, 1907−1920 and references therein. (b) Iyer, K. R.; Jones, J. P.; Darbyshire, J. F.; Trager, W. F. *Biochemistry* **1997**, *36*, 7136−7143. (c) Manchester, J. I.; Dinnocenzo, J. P.; Higgins, L.; Jones, J. P. *J. Am. Chem. Soc.* **1997**, *119*, 5069−5070.

(18) When we checked the percent of **1**-^{18}O generated in the labeled $H_2{}^{18}O$ experiments by carrying out the catalytic epoxidation of cyclohexene with $[Fe^{III}(TPFPP)]^+$ and PhIO under the identical conditions of the toluene hydroxylation, we found that cyclohexene oxide contains 75% ^{18}O. This result indicates that 75% of **1** is ^{18}O-labeled.

(19) (a) Song, R.; Sorokin, A.; Bernadou, J.; Meunier, B. *J. Org. Chem.* **1997**, *62*, 673−678. (b) Sorokin, A.; Meunier, B. *Eur. J. Inorg. Chem.* **1998**, 1269−1281.

(20) Higuchi, T.; Satake, C.; Hirobe, M. *J. Am. Chem. Soc.* **1995**, *117*, 8879−8880.

(21) Khavasi, H. R.; Davarani, S. S. H.; Safari, N. *J. Mol. Catal. A: Chem.* **2002**, *188*, 115−122.

(22) (a) Nam, W.; Valentine, J. S. *J. Am. Chem. Soc.* **1993**, *115*, 1772−1778. (b) Bernadou, J.; Fabiano, A.-S.; Robert, A.; Meunier, B. *J. Am. Chem. Soc.* **1994**, *116*, 9375−9376. (c) Lee, K. A.; Nam, W. *J. Am. Chem. Soc.* **1997**, *119*, 1916−1922. (d) Groves, J. T.; Lee, J.; Marla, S. S. *J. Am. Chem. Soc.* **1997**, *119*, 6269−6273. (e) Bernadou, J.; Meunier, B. *Chem. Commun.* **1998**, 2167−2173. (f) Meunier, B.; Bernadou, J. *Struct. Bonding* **2000**, *97*, 1−35.

(23) Saltzman, H., Sharefkin, J. G., Eds. *Organic Synthesis;* Wiley: New York, 1973; Collected Vol. 5, p 658.

unambiguously that the oxygen in oxygenated products derives from the iron-oxo intermediates, not from molecular oxygen.

Experimental Section

Kinetic Studies and Product Analysis. In general, high-valent iron(IV)-oxo porphyrin π-cation radicals were prepared by adding 1.3 equiv of *m*-CPBA (2 mM, diluted in 50 μL of CH_2Cl_2) to reaction solutions containing their corresponding iron(III) porphyrin triflates (1.5 mM) in a solvent mixture (0.5 mL) of CH_2Cl_2 and CH_3CN (200:1) in a 0.1-cm UV cell at −80 °C. Then, appropriate amounts of substrates (diluted in 100 μL CH_2Cl_2) were added to the UV cell, and spectral changes of the intermediate were directly monitored by a UV−vis spectrophotometer. Rate constants, k_{obs}, were determined by pseudo-first-order fitting of the decrease of absorption bands at 660 nm for **1**, 665 nm for **2**, and 680 nm for **3**. All the rate constants are averages of at least three determinations.

Product analysis was performed by injecting reaction solutions directly into GC and GC−MS. Product yields were determined by comparison with standard curves of known authentic samples and decane as an internal standard. The source of oxygen in oxygenated products was determined by preparing ^{18}O-labeled $[(TPFPP)^{+\bullet}Fe^{IV}(^{18}O)]^+$ (**1**-^{18}O) and using the intermediate directly in the hydroxylation of toluene. To increase the accuracy of the product analysis, the hydroxylation of toluene was performed under catalytic conditions by adding PhI^{18}O, which was prepared by treating PhIO (10 mM, diluted in 50 μL CH_3OH) with $H_2{}^{18}O$ (10 μL, 0.52 mmol, 95% ^{18}O enriched), into a reaction solution containing Fe(TPFPP)(OTf) (2 mM) and toluene (0.2 M) in a solvent mixture (0.5 mL) of CH_2Cl_2 and CH_3CN (200:1) at 25 °C. Then, the reaction mixture was stirred for 0.5 h and directly analyzed by GC−MS. ^{16}O and ^{18}O compositions in 2-methylbenzoquinone were analyzed by the relative abundances of the following mass peaks: m/z = 122 (M), 124 (M + 2), and 126 (M + 4) for 2-methylbenzoquinone (see Scheme 2). The reaction procedures for cyclohexene epoxidation were the same as described for the toluene hydroxylation, and the ^{16}O and ^{18}O compositions in cyclohexene oxide were determined by the relative abundances of the mass peaks at m/z = 83 and 97 for ^{16}O and m/z = 85 and 99 for ^{18}O.

Acknowledgment. This research was supported by the Creative Research Initiative Program of MOST/KOSEF (to W.N.) and the Korea University Grant (to H.G.J.).

Supporting Information Available: General experimental conditions, Figure S1 for the structure of iron(III) porphyrin complexes, and Figure S2 for the determination of second-order rate constants. This material is available free of charge via the Internet at http://pubs.acs.org.

JO070557Y